Standard penetration tests in clays derived from weathered Jurassic mudstones in central England

Kevin Briggs[1*], Yuderka Trinidad González[2], William Powrie[1], Simon Butler[3], Nick Sartain[4]

[1] *Faculty of Engineering and Physical Sciences, University of Southampton, Southampton, SO17 1 BJ, UK*

[2] *Department of Civil, Construction, and Environmental Engineering, Iowa State University, Ames, IA, United States*

[3] *HS2 Ltd (seconded from AtkinRéalis), Birmingham, UK*

[4] *Arup, Birmingham, UK*

ORCID ID: KMB, 0000-0003-1738-9692; YATG, 0000-0003-3715-9712; WP, 0000-0002-2271-0826

*Corresponding author (e-mail: K.Briggs@soton.ac.uk)

Abstract:

Standard Penetration Tests (SPTs) are widely used in the UK for ground profiling and empirical correlation with geotechnical properties and parameters. In particular, Stroud (1974) relates SPT N-values to undrained shear strength through an average coefficient at individual locations. Coefficients have been published for clay-rich tills and mudstone formations. However, few studies have utilised statistically useful datasets (>30 samples) or quantified the variability of the observations relative to the average coefficient.

This paper investigates these issues with reference to large datasets that were obtained from outcrops of weathered Jurassic mudstones in central England as part of a commercial ground investigation for the High Speed Two (HS2) railway. Data pairs from triaxial tests and SPTs located in close proximity ($\pm$1 m vertically, in the same borehole) were used to compare undrained shear strength and SPT N_{60}-values, and explore the variability of the observations relative to the average coefficient.

The results show that the average coefficients derived for each geological formation were close to published relationships. However, statistical analyses showed dispersion about the mean. Locally low values in the 5% fractile were between 15% and 50% of the mean value. Therefore, average coefficients are informative, but they should be used with caution.

Introduction

Standard Penetration Tests (SPTs) are widely used in the UK for ground profiling, in-situ testing and for empirical correlations with geotechnical properties and parameters (Clayton, 1995). They complement more rigorous sampling and laboratory testing by providing many measurements, and therefore a large sample size, at minimal cost (Reid & Taylor, 2010). The SPT measures the number of hammer blows (the blowcount or *N*-value) required to drive a split barrel sampler through a seating drive of 150 mm and a main drive of 300mm using a 63.5 kg impact weight falling from 760 mm height (British Standards Institution, 2005). The SPT procedure was not standardised at its inception (Terzaghi & Peck, 1948) and it is not fully standardised internationally (Skempton, 1986; Clayton, 1995), but current UK practice is defined by BS EN ISO 22476-3:2005+A1:2011 (British Standards Institution, 2005).

The SPT has been used to estimate a range of geotechnical properties (e.g. strength, stiffness and compressibility) for granular and fine soils, and weak and weathered rocks (Clayton, 1995). The empirical nature of these relationships requires them to be calibrated for specific soil and rock types (Clayton, 1995). Site specific calibration may be needed for stiff clays derived from weathered mudstones, where the influence of weathering alters the structure, fabric and geotechnical properties of the clays from those of the parent mudstone (Chandler, 1972; Cripps & Taylor, 1981; Briggs et al. 2022).

In the UK, a number of correlations have been developed using an average coefficient to relate SPT *N*-values with the undrained shear strength of clay-like materials in fissured, clay-rich tills and in mudstone formations (Table 1). These are generally based on the Stroud (1974) relationship:

$$S_{u,UU} = f_1 \times N$$

Equation 1

where $S_{u,UU}$ is the undrained shear strength (kPa) as measured in unconsolidated undrained (UU) triaxial compression tests, f_1 (kPa) is a coefficient that is independent of depth and discontinuity spacing and N is the SPT *N*-value. Stroud (1974) and Stroud and Butler (1975) showed that the numerical value of the f_1 coefficient varied with the plasticity index of the clays at the sites they examined, but this has not been shown for other soil types (Sowers, 1954; Reid & Taylor, 2010; Sivrikaya & Toğrol, 2006). In many cases the f_1 coefficient was determined across individual sites or for multiple sites in a single geological formation as an averaged value, assuming that both the shear strength and SPT *N*-values increased linearly with depth at the same gradient (Stroud 1974, Stroud & Butler, 1975; Stroud, 1989; Sivrikaya & Toğrol, 2006; Reid & Taylor, 2010). In other cases, the f_1 coefficient was determined from the one-to-one comparison of individual pairs of triaxial test and SPT data located in close proximity, and then averaged to determine a single value for an individual site or geological formation (White et al. 2019; Crispin et al. 2024). White et al. (2019) noted that SPT samplers have changed over time and will affect the measured f_1 coefficient.

These previous studies have shown that SPT *N*-values can be used to estimate the undrained shear strength of clays and mudstones, but the relationship is relatively weak and correlations should be used with great care (British Standards Institution, 2020). However, SPTs can be used to generate large amounts of qualitative data relatively quickly and cheaply. In addition, they are less sensitive to localised features in the ground (e.g. individual fissures) that may reduce the strength of triaxial samples. Therefore, they continue to be routinely undertaken during ground investigations to complement laboratory testing (Griffiths, 2019; AGS, 2020). Statistical value can be obtained from SPTs because they are often numerous relative to other types of geotechnical measurement. The statistical interpretation of many observations can complement data evaluation based on engineering judgement by allowing the calculation of mean values and their variation for the population. This can help to avoid common mistakes in the application of engineering judgement as associated with overconfidence, a poor understanding of representativeness based on limited observations, and ignorance of prior probabilities or base rates (Tversky & Kahneman, 1974; Baecher & Christian, 2003).

This study examines SPT data obtained in clay soils derived from weathered mudstones in Jurassic-aged outcrops in central England. The work was undertaken in response to (i) the limited published data for SPT correlations in clays derived from these weathered mudstones, (ii) the availability of statistically useful datasets (>30 samples) for the one-to-one comparison of SPTs and triaxial testing data, and (iii) standardisation of the SPT (e.g. British Standards Institution, 2005) and weathering classification systems (British Standards Institution, 2020) to improve the reliability of SPT and borehole logger descriptions, relative to earlier studies.

The aims were to (i) explore SPT correlations with undrained shear strength from a one-to-one comparison of SPT N_{60}-values and triaxial testing data located in close proximity, (ii) quantify the expected variability of the correlations relative to the average, and (iii) compare these with published correlations for similar geological materials.

Geology

The ground investigation included a total length of 47 km of outcrops of the Oxford Clay Formation (Ancholme Group), Whitby Mudstone Formation (Lias Group) and Charmouth Mudstone Formation (Lias Group) (Figure 1). The geology comprised Jurassic mudstones that had been overconsolidated and then subjected to glacial, periglacial and contemporary weathering to different extents in the Quaternary period (Murton & Ballantyne, 2017). Material specific weathering schemes for the Oxford Clay and Lias Clay are summarised in Norbury (2020). These conform with BS 5930:2015+A1:2020 'Approach 4', for weak rocks (British Standards Institution, 2020). The Norbury (2020) weathering classifications include unweathered (Class A) mudstone, partially weathered mudstone (Class Ba), partially weathered clay (Class Bb), distinctly weathered clay (Clay C), destructured clay (Class D) and reworked clay (Class E).

The first group of SPTs was located along a 12.4 km length in an outcrop of the Oxford Clay Formation (Ancholme Group) to the south of Buckingham, Buckinghamshire (Figure 1). The Oxford Clay Formation (Ancholme Group) of the East Midlands Shelf comprises grey, clay-rich mudstones deposited in shallow marine conditions ~161–156 myr ago. These form a consistent, highly bedded fabric with horizontal laminations and limited fissuring (Parry, 1972; Russell & Parker, 1979). The outcrop is generally ~65 m thick in Buckinghamshire (Sumbler, 2002; Price, 2018). Weathered clay was encountered to approximately 7.5 m bgl. This compares with the Oxford Clay Formation across central England, which includes weathered clay (Class Bb-E) to between 3 m bgl (Hird & Pierrepoint, 1997) and 7.5 m bgl (Russell & Parker, 1979), with unweathered clay below.

The second and third groups of SPTs were located along a 34.4 km length in outcrops of the Whitby Mudstone Formation and Charmouth Mudstone Formation (Lias Group) located to the east and the north of Banbury, Oxfordshire (Figure 1). The Whitby Mudstone Formation and Charmouth Mudstone Formation (Lias Group) of the East Midlands Shelf comprise grey, clay-rich mudstones and siltstones formed in shallow marine conditions ~174-199 myr ago (Cox et al. 1999; Hobbs et al. 2012). The ground investigation data showed a gradational weathering profile of clay (Class Bb-E) and weathered mudstone (Class Ba) extending to approximately 12 m bgl, with unweathered (Class

A) mudstone below (Briggs et al. 2022). The ground investigation data showed that the weathered clay (Class Bb-E) in the Whitby Mudstone Formation outcrop extended to approximately 8 m bgl. This compares with measurements in the Whitby Mudstone Formation elsewhere at Culworth, Northamptonshire (Chandler, 1972).

The ground profiles at the borehole locations shown in Figure 1 were influenced by glacial and periglacial weathering (Moore et al. 2022). The Oxford Clay Formation north of Twyford was glaciated at least once in the last 450 kyr (Clark et al. 2004; Murton et al. 2015) and then experienced periglacial conditions. The Lias Group outcrop east of Banbury and towards Southam was glaciated in the last 450 kyr and experienced periglaciation conditions during the Last Glacial Maximum, approximately 26-19 kyr ago (Shotton, 1953; Clark et al. 2004). This has altered the engineering properties of the ground. For example, Chandler (1972) showed that greater weathering correlated with increased oxidation, increased moisture content and reduced undrained shear strength in the Whitby Mudstone Formation. Coulthard & Bell (1993) showed increase fissuring, moisture content and reduced undrained shear strength in weathered samples from the Charmouth Mudstone Formation. Russell & Parker (1979) showed undrained shear strength reduction in the Oxford Clay Formation due to weakening of interparticle bonds, the solution of diagenetic minerals and the degradation of illite in weathered samples.

Method

Ground investigation data including borehole records, soil classification tests, unconsolidated undrained (UU) triaxial tests and Standard Penetration Tests (SPTs) were obtained from a ground investigation for the High Speed Two (HS2) railway between London and Birmingham. The ground investigation was undertaken by multiple contractors between 2017 and 2020. It was compiled into the digital AGS Data Format (Chandler et al. 2006).

Triaxial test data

Undrained shear strength ($S_{u,UU}$) values were obtained from unconsolidated, undrained (UU) triaxial tests undertaken according to BS1377-7:1990 (British Standards Institution, 2010), together with associated data including initial moisture content and bulk density. These data were filtered to extract results from tests on intact, 100 mm diameter, 200 mm high clay ($S_{u,UU}$ < 300 kPa) samples from less than 10 m bgl. Most of the samples were obtained using cable percussion drilling and a thin wall open drive tube sampler. They were tested at a cell pressure equal to the estimated in situ total vertical stress. Data from other strata or test types were excluded from the analyses. The triaxial data were compared with borehole records including the strata descriptions and the visually-assessed weathering class. The weathering profile was classified during the commercial ground investigation using BS 5930:2015+A1:2020 'Approach 4', for weak rocks (British Standards Institution, 2020).

SPT data

SPTs were undertaken using either a cable percussive drill rig or crawler-mounted drill rig, in accordance with BS EN ISO 22476-3:2005+A1:2011 (British Standards Institution, 2005). Data were filtered to exclude SPTs where the total number of blows needed to achieve the main drive of 300 mm (following a seating drive of 150 mm) was greater than 50. This is the limit where drilling can finish (British Standards Institution, 2005) and is sometimes described as 'refusal'. The raw SPT *N*-values were adjusted to a reference energy ratio of 60% (N_{60}) using:

$$N_{60} = \left({}^{E_r}/_{60}\right) \times N$$

Equation 2

where the *N*-value (*N*) is the number of hammer blows required to achieve a 300 mm drive length and E_r is the energy ratio of the test equipment for each test, as recorded in the borehole log.

Pairing of triaxial and SPT data

The borehole records show that the triaxial samples were all from weathered clay strata (Class Bb-E), which is consistent with the selection criteria for the data points of $S_{u,UU}$ < 300 kPa. The triaxial test data were paired with SPT data located within close vertical proximity (±1 m vertically, in the same borehole). Huang et al. (2022) examined the spatial variability of the Oxford Clay, Whitby Mudstone and Charmouth Mudstone Formations in the vertical direction based on cone penetration test (CPT) data. The average scale of fluctuation (that is, the distance over which material properties are correlated) was calculated for each formation as 0.43 m, 0.33 m and 0.33 m respectively. This suggests that ideally, triaxial and SPT data would have been compared for samples located within 0.33 m vertical distance. However, this was not possible owing to the length of the seating (150 mm) main (300 mm) drives of the SPT. Triaxial and SPT data were therefore considered to be in close proximity when they were located within the same borehole and separated by less than 1 m vertically, centre to centre (that is, from the centre of the triaxial sample to the centre of the main SPT drive). A total of 135 data pairs, extending up to 7.5 m bgl in weathered clay, were created in this way. There were no SPT and triaxial pairs from greater depths because either (i) SPT measurements were not undertaken in the stronger clays and mudstones at depth, or (ii) the material transitioned to mudstone ($S_{u,UU}$ > 300 kPa), which was not included in the analyses. The data were not categorised by weathering class because this created categories with a low number of data pairs that were unsuitable for regression analyses.

Table 2 shows that the SPTs were linked to 48 UU triaxial tests with soil classification data, including measurements of the liquid limit (%), plastic limit (%) and plasticity index (%). Figure 2 shows that the triaxial samples of weathered clay from the Oxford Clay (OXC_w), Whitby Mudstone (WHM_w) and Charmouth Mudstone Formations ($CHAM_w$) were mostly high plasticity, in agreement with Hird & Pierpoint (1997) and Briggs et al. (2022). The properties of the ground at shallow depth (the SPTs were up to ~7 mbgl) were depth-dependant, rather than elevation-dependant. This is in agreement with soil classification and strength measurements at shallow depth in the Charmouth Mudstone Formation (Briggs et al. 2024; Briggs et al. 2025) and the Oxford Clay Formation (Parry, 1972; Russell & Parker, 1979).

Figure 3, Figure 4 and Figure 5 show the profiles of undrained shear strength (kPa) and SPT N_{60}-values with depth for the data pairs, categorised by geological formation. The Figures show an increase in both undrained shear strength (kPa) and SPT N_{60}-value with depth. However, there is significant scatter, as shown by the descriptive statistics of the mean (μ), standard deviation (σ) and coefficient of variation (*COV*) (Table 3). The coefficient of variation (*COV*) is a relative measure of dispersion that indicates the magnitude of the standard deviation in relation to the mean ($COV = \sigma/\mu$). It is used in geotechnical engineering (Phoon and Kulhawy, 1999) but it is not an intrinsic statistical property (Phoon et al. 2022). Phoon and Kulhawy (1999) provide indicative values of the COV of geotechnical design parameters, including typically 30-55% for undrained shear strength measured using an in-situ shear vane.

The scatter in the undrained shear strength (kPa) profiles of the weathered mudstones (Figure 3, Figure 4 and Figure 5) is greater than in equivalent measurements in the London Clay Formation by Stroud (1974). This difference was also shown by Stroud (1974), who suggested that the measurements at depth in the Oxford, Kimmeridge and Lias Clays may underestimate the in-situ strength. This may result from disturbance, fracturing and hence weakening of recovered samples, which is more likely in the relatively brittle, Jurassic-aged mudstones than in younger or more plastic clays such as those of the London Clay Formation. This is supported by the undrained shear strength (kPa) data in Figure 3, Figure 4 and Figure 5, which include a number of strength measurements of less than 75 kPa that are present throughout the depth profile.

Interpretation

Many correlations between SPT *N*-values and undrained shear strength use a single coefficient, such as f_1, for each site or geological formation (Table 1). In this study, a single coefficient was first determined for each of the individual data pairs (f_p) shown in Table 2 using:

$$f_p = S_{u,UU}/N_{60}$$

Equation 3

where $S_{u,UU}$ is the undrained shear strength measured in an unconsolidated undrained (UU) triaxial compression test, and N_{60} is the paired SPT N_{60}-value (Equation 2). There were some low SPT N_{60}-values (<12) at shallower depth (1-2 m bgl) that were associated with large $S_{u,UU}$ values and were deemed unreliable. This may result from the pairing of tests up to 1 m apart vertically, which had the greatest effect at shallow depth. Therefore, a threshold was set to remove pairs with SPT N_{60}-values < 12 from the interpretation and statistical analyses.

Coefficients were then calculated for each geological formation using two methods:

1. Linear regression was used to calculate the f_1 coefficient with the best fit to the triaxial and SPT data pairs in each geological formation. This can be used as a predictor of undrained shear strength from SPT *N*-values, as shown for the published relationships in Table 1.
2. Individual f_p coefficients for the triaxial and SPT data pairs were fitted to a Gaussian (normal) probability distribution function for each geological formation. This was then used to determine the average (μ) values and the distribution of the individual f_p coefficients. This can be used to assess both the most probable (average) value of the f_p coefficient in a geological formation ($f_{p,\mu}$) and the probability of higher or lower values at specific thresholds, for example at the 95% fractile ($f_{p,95}$) or 5% fractile ($f_{p,5}$).

Linear regression through the origin (an average trendline model) was used to relate the undrained shear strength (the outcome variable) to the SPT N_{60}-value (the predictor variable) using a single f_1 coefficient. This was used to find the best fit f_1 coefficient for each geological formation, for comparison with published relationships (Table 1). A linear regression through the origin was obtained by least-squares methods to obtain a single coefficient relating two variables, without the constant term required for ordinary least-squares regression. The removal of the constant term can worsen the best fit to the data but is appropriate when the constant has no physical meaning (Eisenhauer, 2003), as in the interpretation of SPT data (Sivrikaya & Toğrol, 2006; Reid & Taylor, 2010). The coefficient of variation (*COV*) for each formation was calculated to compare the dispersion of the actual undrained shear strength data from the model values. The coefficient of variation (*COV*) was calculated by dividing the standard deviation of the residuals from the regression model for the undrained shear strength by the mean of the undrained shear strength. In addition, the Mean Absolute Percentage Error (MAPE) was calculated for each formation to provide a simple quantitative measure of the regression model accuracy (De Myttenaere et al. 2016). The MAPE is the average of the absolute percentage errors between the undrained shear strength data and that calculated using the f_1 regression coefficients.

A probability density function was used to calculate the average values for the f_p coefficients in each geological formation, and their distribution (that is, the range of f_p values and their probability of occurrence). The f_p coefficient (Equation 3) was calculated for each SPT and triaxial pair (n =135) and categorised by geological formation. The results were plotted as a probability histogram and fitted to a Gaussian probability density function, which has been used previously to fit both soil strength and SPT data (Baecher & Christian, 2003). The probability histogram and probability density function were used to determine the average (μ) values of the f_p coefficients in each geological formation. This method was most reliable for the larger (n > 30) datasets of the Oxford Clay Formation (n = 70) and Charmouth Mudstone Formation (n = 53). A probability histogram and probability density function were not generated for the Whitby Mudstone Formation owing to the small size of the dataset (n = 12). The variance (σ^2) and standard deviation (σ) were calculated for each geological formation, to measure the variability of the f_p coefficients. From this, the coefficient of variation (*COV*) was calculated, as were upper and lower values of f_p in the 95th percentile ($f_{p,95}$) and 5th percentile ($f_{p,5}$) respectively. The 5th percentile value of the f_p coefficient was calculated to show the lowest value, with a probability of being exceeded in 95% of cases.

Table 2 shows that 48 SPTs were paired with UU triaxial tests and soil classification data. These pairings were used to examine the relationship between the f_1 coefficient and the plasticity index shown in Stroud (1974). The f_p coefficient (Equation 3) was calculated for each of the SPT and triaxial pairs and compared with the plasticity index of the triaxial sample. The mean values of f_p for each formation ($f_{p,\mu}$) and the plasticity index were calculated for the Oxford Clay and Charmouth Mudstone Formations. These were compared with f_1 values for the Oxford Clay and Whitby Mudstone Formations given in Stroud (1974).

Results

Figure 6 compares the SPT N_{60}-values and undrained shear strength measurements in the weathered clays, categorised by geological formation. The trend lines show that the undrained shear strength increased with the SPT N_{60}-value. The f_1 coefficients range between 2.98 (for the WHM_w) and 3.71 (for the $CHAM_w$). They are therefore close to the published values for the same geological formations shown in Table 1, which range from 3.3 to 5.6 in the OXC_w and 4.0 in the WHM_w (Stroud, 1974). The coefficient of variation (COV) values for the f_1 coefficients in Table 4 range from 36% (for the $CHAM_w$) to 55% (for the OXC_w). This is greater than for the SPT and triaxial data (Table 3) and towards the upper limit of COV for geotechnical parameters given by Phoon & Kulhawy (1999). The MAPE for the f_1 coefficients ranges from 28% (for the $CHAM_w$) to 55% (for the OXC_w and WHM_w), showing that the regression models were more accurate for the $CHAM_w$ than for the OXC_w and WHM_w.

Figure 7 shows the probability density histograms of the f_p coefficient for individual samples in the OXC_w and $CHAM_w$, fitted to a Gaussian (normal) probability density function. From these, the mean coefficients (μ) can be used to estimate the mean coefficients for each formation ($f_{p,\mu}$). The data from the WHM_w were not a good fit to the Gaussian PDF due to the small sample size (n = 12) and are therefore not shown. Figure 7 shows that the $f_{p,\mu}$ coefficients are greater than those derived from linear regression through the origin (Figure 6) but lie within the range of published values shown in Table 1. Table 4 includes the coefficient of variation (COV) of the $f_{p,\mu}$ coefficients. This shows that there was the least variation about the mean and the best fit to the Gaussian PDF for the $CHAM_w$ data pairs. Therefore, the $f_{p,\mu}$ coefficient for the $CHAM_w$ is the most useful of the three geological formations considered. Table 4 shows upper and lower values of f_p in the 95th percentile ($f_{p,95}$) and 5th percentile ($f_{p,5}$) respectively for each geological formation. The values for $CHAM_w$, which had the best fit to the Gaussian PDF, show that while the mean $f_{p,\mu}$ coefficient for the formation is 4.09, this ranges between a minimum ($f_{p,5}$) of 1.90 and a maximum ($f_{p,95}$) of 6.28. The range of minimum ($f_{p,5}$) and maximum ($f_{p,95}$) coefficients is greater than this for the OXC_w, but these values are less reliable than for the $CHAM_w$ owing to the poorer model fit (i.e. the Gaussian PDF).

Figure 8 shows the f_p coefficient derived from the individual SPT and triaxial pairs plotted as a function of the plasticity index of the sample, where available (n = 48). The results are categorised by geological formation (OXC_w, WHM_w and $CHAM_w$), with mean values for the OXC_w and $CHAM_w$ ($f_{p,\mu}$) shown in black. These are compared with the mean values from individual sites (f_1) measured by Stroud (1974) in comparable strata and the Stroud (1974) trend line relating the f_1 coefficient to plasticity index. The $f_{p,\mu}$ coefficients for the OXC_w and $CHAM_w$ lie close to those measured by Stroud (1974) in the same geological formations. However, inspection of the individual f_p results shows scatter that does not agree with the Stroud (1974) trendline. Therefore, for these data, any relationship between the $f_{p,\mu}$ coefficient and plasticity index is small relative to the variability in the individual data pairs (that is, in f_p).

Discussion

The Stroud (1974) coefficient (f_1) gives the best-fit slope from a linear regression of undrained shear strength $S_{u,UU}$ against N_{60} for each geological formation (Table 1). However, this study also computes an individual coefficient (f_p) for each data pair and the distribution of these values in each formation. A normal distribution (Gaussian) was fitted to the f_p values, allowing the derivation of mean coefficients ($f_{p,\mu}$) and percentile-based values such as the 5th and 95th percentile values, ($f_{p,5}$ and $f_{p,95}$). The f_1 coefficients reflect a regression relationship that is influenced by the spread and weighting of data across the range of N_{60}, while $f_{p,\mu}$ is the arithmetic mean average of individual data pairs. Therefore, the coefficients can have similar, but not always identical values. The percentile values derived from the histogram of f_p, coefficients allow flexibility to choose appropriate coefficients for probabilistic design by re-writing Equation 3:

$$S_{u,UU} = f_{p,pc} \times N_{60}$$

Equation 4

where $S_{u,UU}$ is the undrained shear strength (kPa), N_{60} is the SPT N_{60}-value and $f_{p,pc}$ (kPa) is a coefficient for the *pc-th percentile* (*pc* is a number from 0 to 100). For example, Figure 9 shows $S_{u,UU}$ values calculated using the mean ($f_{p,\mu}$) and the percentile-based $f_{p,5}$ *and* $f_{p,95}$ coefficients in Table 4 for the Charmouth Mudstone Formation ($CHAM_w$). They are compared to the unconsolidated undrained (UU) triaxial compression tests (Figure 5). As expected, the shear strength values calculated using $f_{p,\mu}$ fall within the range of the triaxial measurements. Undrained shear strength values calculated using $f_{p,5}$ provide more conservative values, while $f_{p,95}$ provides higher values.

Conclusions

The Stroud (1974) approach can be used to derive individual (f_p) and formation-wide (f_1) coefficients from individual pairs of SPTs and unconsolidated undrained (UU) triaxial tests in weathered clays ($S_{u,UU}$ < 300kPa). Data were examined for SPT and triaxial data pairs located in close proximity (±1 m vertical distance in the same borehole) in weathered clays from the Oxford Clay (OXC_w), Whitby Mudstone (WHM_w) and Charmouth Mudstone Formations ($CHAM_w$) in central England. The following conclusions can be drawn:

1. Published f_1 coefficients are generally applicable to the weathered mudstones considered in this study to obtain average values of undrained shear strength from SPT blow count data. The results show that the f_1 coefficients derived using linear regression through the origin are close to published f_1 coefficients for stiff clays and weak mudstones (Table 1). However, the f_1 coefficients provide average values but do not provide information about the dispersion from the mean, which can be large.
2. There is high variability in both the undrained shear strength (kPa) and SPT N_{60}-values in the weathered mudstones, which may result from disturbance, fracturing and therefore weakening during sampling and/or testing. The f_1 coefficients represent average values, but the results from individual pairs show that there is dispersion about the mean, with coefficients of variation (COV) between 36% and 55% and Mean Absolute Percentage Errors (MAPE) between 28% and 55%. This supports the assertion that SPT *N*-values should be used with caution when estimating the undrained shear strength of brittle materials such as stiff clays and weak mudstones (Stroud, 1974; Reid & Taylor, 2010; British Standards Institution, 2020).
3. When the sample size is statistically useful ($n > 30$), a Gaussian probability density function (PDF) can be fitted to the f_p coefficients derived from individual SPT and triaxial pairs. This provides an interpretation that accounts for the range of likely f_p coefficients including the probability of lower-bound, average and upper-bound values. This allows lower-bound and upper-bound values to be considered more explicitly than when using linear regression. The results show that lower-bound f_p coefficients can be much lower than the average values. For example, results for the Charmouth Mudstone Formation ($CHAM_w$) show that the f_p coefficient reduced from a mean value of $f_{p,\mu} = 4.09$, to a lower bound value of $f_{p,5} = 1.90$. A greater reduction to approximately 15 % of the mean value was shown for the Oxford Clay Formation (OXC_w).
4. The $f_{p,\mu}$ coefficient for each geological formation varied slightly with plasticity index, consistent with (f_1) coefficients in other mudstone strata such as London Clay (Stroud, 1974; Stroud, 1989; White et al. 2019). However, the f_p coefficient for individual SPT and triaxial pairs showed a large dispersion from the trend. Therefore, while it may be acceptable to use formation specific coefficients for the weathered clays that were considered at these sites (as in the first conclusion), the evidence from this study does not support the use of model coefficients based on plasticity index.

Acknowledgements

Thank you to HS2 Ltd and their contractors for sharing the ground investigation data and providing supporting information. Thank you to the reviewers for their helpful comments.

Funding

Kevin Briggs is supported by the Royal Academy of Engineering and HS2 Ltd under the Senior Research Fellowship scheme (RCSRF1920\10\65). This paper is an output from ACHILLES, an Engineering and Physical Sciences Research Council (EPSRC) programme grant led by Newcastle University (EP/R034575/1).

Data availability

The datasets generated during this study are available from the University of Southampton repository at https://doi.org/10.5258/SOTON/D3369.

References

AGS, 2020. 'Ground investigation – Is it time for change?' *AGS Magazine - June/July 2020*. Association of Geotechnical and Geoenvironmental Specialists, UK.

Baecher, G.B. and Christian, J.T., 2005. *Reliability and statistics in geotechnical engineering*. John Wiley & Sons.

Briggs, K.M., Blackmore, L., Svalova, A., Loveridge, F.A., Glendinning, S., Powrie, W., Butler, S. and Sartain, N., 2022. The influence of weathering on index properties and undrained shear strength for the Charmouth Mudstone Formation of the Lias Group at a site near Banbury, Oxfordshire, UK. *Quarterly Journal of Engineering Geology and Hydrogeology*, *55*(3), pp.qjegh2021-066.

Briggs, K.M., Trinidad González, Y., Powrie, W., Butler, S. and Sartain, N., 2024. Quantifying CPT cone factors in clays derived from weathered mudstone. *Quarterly Journal of Engineering Geology and Hydrogeology*, 57(1), pp.qjegh2023-014.

Briggs, K.M., González, Y.T., Meijer, G.J., Powrie, W., Butler, S. and Sartain, N., 2025. In situ shear modulus reduction with strain in stiff fissured clays and weathered mudstones. *Canadian Geotechnical Journal*, 62, pp.1-19.

British Geological Survey. 2020. The BGS Lexicon of Named Rock Units [online]. Keyworth, Nottingham. Available from https://www.bgs.ac.uk/technologies/the-bgs-lexicon-of-named-rock-units/

British Standards Institution, 1990. BS 1377-7:1990. *Methods of test for soils for civil engineering purposes. Shear strength tests (total stress)*, BSI, London.

British Standards Institution, 2013. BS EN 1997-1:2004+A1:2013. *Eurocode 7: Geotechnical design. Part 1: General rules,* BSI, London.

British Standards Institution, 2005. *BS EN ISO 22476-3:2005+A1:2011. Geotechnical investigation and testing - Field testing - Part 3: Standard penetration test*, BSI, London.

British Standards Institution, 2010a. BS 1377-2:1990. *Methods of test for soils for civil engineering purposes. Classification tests*. BSI, London.

British Standards Institution, 2010b. BS 1377-7:1990. *Methods of Test for Soils for Civil Engineering Purposes. Shear Strength Tests (Total Stress)*. BSI, London

British Standards Institution, 2014. BS EN ISO 17892-1:2014. *Geotechnical investigation and testing. Laboratory testing of soil. Determination of water content.* BSI, London.

British Standards Institution, 2020. *BS 5930:2015+A1:2020. Code of Practice for Ground Investigations*. BSI, London.

Cox, B. M., Sumbler, M. G. and Ivimey-Cook, H. C. 1999. *A formational framework for the Lower Jurassic of England and Wales (onshore area).* British Geological Survey Research Report, RR/99/01.

Crispin, J.J., Gilder, C.E.L. and Vardanega, P.J. 2024. Review of SPT-undrained shear strength correlation for UK soil deposits. In *Proceedings of the XVIII European Conference on Soil Mechanics and Geotechnical Engineering*. Lisbon, Portugal. ISBN 978-032-54816-6.

Chandler, R.J., 1972. Lias clay: weathering processes and their effect on shear strength. *Geotechnique*, *22*(3), pp.403-431.

Chandler, R.J., Quinn, P.M., Beaumont, A.J., Evans, D.J. and Toll, D.G., 2006. Combining the power of AGS and XML: AGSML the data format for the future. In *GeoCongress 2006: Geotechnical Engineering in the Information Technology Age* (pp. 1-6).

Coulthard, J.M. and Bell, F.G., 1993. The engineering geology of the lower Lias clay at Blockley, Gloucestershire, UK. *Geotechnical & Geological Engineering*, 11, pp.185-201.

Cripps, J.C. and Taylor, R.K., 1981. The engineering properties of mudrocks. *Quarterly Journal of Engineering Geology and Hydrogeology*, *14*(4), pp.325-346.

Clark, C.D., Gibbard, P.L. and Rose, J. 2004. Pleistocene glacial limits in England, Scotland and Wales. In: *Quaternary Glaciations – Extent and Chronology*, Part I: Europe. Elsevier, Amsterdam.

Clayton, C.R.I. 1995. *The standard penetration test (SPT): methods and use* CIRIA. 129pp.

De Myttenaere, A., Golden, B., Le Grand, B., & Rossi, F. , 2016. Mean absolute percentage error for regression models. *Neurocomputing*, 192, 38-48.

Eisenhauer, J.G., 2003. Regression through the origin. *Teaching statistics*, *25*(3), pp.76-80.

Griffiths, J.S., 2019. Advances in engineering geology in the UK 1950–2018. *Quarterly Journal of Engineering Geology and Hydrogeology*, *52*(4), pp.401-413.

Hird, C.C. and Pierpoint, N.D., 1997. Stiffness determination and deformation analysis for a trial excavation in Oxford Clay. *Geotechnique*, *47*(3), pp.665-691.

Hobbs, P.R.N., Entwisle, D.C., Northmore, K.J., Sumbler, M.G., Jones, L.D., Kemp, S., Self, S., Barron, M. and Meakin, J.L. 2012. *Engineering Geology of British Rocks and Soils: Lias Group*. British Geological Survey Internal Report OR/12/032. British Geological Survey, Keyworth, Nottingham, UK

Huang, W., Dijkstra, T., Loveridge, F., Hughes, P., Blake, A.P., Dobbs, M. and Gonzalez, Y.T., 2022, December. Spatial variability of London Clay using CPT and SPT data. In *8th International Symposium on Geotechnical Safety and Risk* (pp. 228-234).

Moore, R., Fish, P., Trinder, S., Czarnomski, C., Dabson, O. and Fitzgerald, R., 2022. Engineering geomorphology of HS2: management of geohazards. *Quarterly Journal of Engineering Geology and Hydrogeology*, 55(4), pp.qjegh2021-122.

Murton, J.B., Bowen, D.Q., Candy, I., Catt, J.A., Currant, A., Evans, J.G., Frogley, M.R., Green, C.P., Keen, D.H., Kerney, M.P., Parish, D., Penkman, K., Schreve, D.C., Taylor, S., Toms, P.S., Worsley, P., and York, L.L., 2015. Middle and Late Pleistocene environmental history of the Marsworth area, south-central England. *Proceedings of the Geologists' Association*, 126, 18-49.

Murton, J.B. and Ballantyne, C.K., 2017. Chapter 5 Periglacial and permafrost ground models for Great Britain. *In*: Griffiths, J.S. & Martin, C.J (eds) *Engineering geology and geomorphology of glaciated and periglaciated terrains: engineering group working party report*. Geological Society, London, Engineering Geology Special Publications, 28(1), pp.501-597.

Nash, D.F.T., Lings, M.L. and Ng, C.W.W., 1996. Observed heave and swelling beneath a deep excavation in Gault clay. In *Geotechnical Aspects of Underground Construction in Soft Ground: Proc. Int. Symposium, London UK* (pp. 191-196). AA Balkema.

Norbury, D.R. 2020. *Soil and Rock Description in Engineering Practice*. 3rd edition. Whittles Publishing, Dunbeath, Caithness, UK.

Parry, R. H. G. 1972. Some properties of heavily overconsolidated Oxford Clay at a site near Bedford. *Geotechnique* 22, No. 3, 485–507, http://dx.doi.org/10.1680/geot.1972.22.3.485

Phoon, K.K. and Kulhawy, F.H., 1999. Evaluation of geotechnical property variability. *Canadian Geotechnical Journal*, 36(4), pp.625-639.

Phoon, K.K., Cao, Z.J., Ji, J., Leung, Y.F., Najjar, S., Shuku, T., Tang, C., Yin, Z.Y., Ikumasa, Y. and Ching, J., 2022. Geotechnical uncertainty, modeling, and decision making. *Soils and Foundations*, 62(5), p.101189.

Prästings, A., Spross, J. and Larsson, S., 2019. Characteristic values of geotechnical parameters in Eurocode 7. *Proceedings of the Institution of Civil Engineers-Geotechnical Engineering*, 172(4), pp.301-311.

Price, S. 2018. *The glacial and periglacial history of a Middle Pleistocene ice-margin of the British Ice Sheet (BIS) in north Buckinghamshire, England and its influence on geotechnical variability*. PhD thesis. University of Cambridge, UK.

Reid, A. and Taylor, J., 2010. The misuse of SPTs in fine soils and the implications of Eurocode 7. *Ground Engineering*. July, 43(7) pp. 28-31.

Russell, D.J. and Parker, A., 1979. Geotechnical, mineralogical and chemical interrelationships in weathering profiles of an overconsolidated clay. *Quarterly Journal of Engineering Geology*, 12(2), pp.107-116.

Shotton, F.W. 1953. The Pleistocene deposits of the area between Coventry, Rugby and Leamington and their bearing upon the topographic development of the Midlands. *Philosophical Transactions of the Royal Society of London*, Series B: Biological Sciences, 237, 209–260, https://doi.org/10.1098/rstb.1953.0004

Sivrikaya, O.S.M.A.N. and Toğrol, E., 2006. Determination of undrained strength of fine-grained soils by means of SPT and its application in Turkey. *Engineering geology*, *86*(1), pp.52-69.

Skempton, A.W., 1986. Standard penetration test procedures and the effects in sands of overburden pressure, relative density, particle size, ageing and overconsolidation. *Geotechnique*, *36*(3), pp.425-447.

Sowers, G.F. 1954. Modern procedures for underground investigations. Proc. ASCE, 80 (Separate 435), 11pp.

Stroud, M.A., 1974. The standard penetration test in insensitive clays and soft rocks. In *Proceedings of the 1st European Symposium on Penetration Testing, Stockholm, Sweden* (Vol. 2, No. 2, pp. 367-375).

Stroud, M.A. and Butler, F.G., 1975. The standard penetration test and the engineering properties of glacial materials. In *Symposium on Engineering Properties of Glacial Materials, Midland Geotechnical Society*.

Sumbler, M. G. 2002. Geology of the Buckingham district a brief explanation of the geological map Sheet 219 Buckingham. Sheet Explanation of the British Geological Survey 1:50 000 Sheet 219 Buckingham (England and Wales).

Terzaghi, K. and Peck, R.B., 1948. Soil Mechanics. *Engineering Practice. John Wiley and Sons, Inc., New York*.

Tversky, A. and Kahneman, D., 1974. Judgment under Uncertainty: Heuristics and Biases: Biases in judgments reveal some heuristics of thinking under uncertainty. *Science*, 185(4157), pp.1124-1131.

White, F., Ingram, P., Nicholson, D., Stroud, M. and Betru, M. 2019. An update of the SPT-cu relationship proposed by M. Stroud in 1974. In: *Proc. of ECSMGE-2019*, Reykjavík, Iceland. doi:10.32075/17ECSMGE-2019-0500

Tables

Table 1: Standard penetration test (SPT) and undrained shear strength ($S_{u,UU}$) correlations in stiff clays and weak mudstones derived from clay-rich units in the UK. The f_1 coefficient is dependent on the plasticity index (PI or I_p) for some overconsolidated clays in Stroud (1974).

Geological Unit*	**Model**	**Model coefficient, f_1 or A_1 (kN/m^2)**	**Reference**
Till (Glacial deposit)	$S_{u,UU} = f_1 \cdot N$	4.5-6.0, decreasing with PI	Stroud & Butler, 1975**
Till (Glacial deposit)	$S_{u,UU} = A_1 \cdot N_{60}$	4.0	Reid & Taylor, 2010
London Clay Formation (Thames Group)	$S_{u,UU} = f_1 \cdot N$ Where f_1 varies by PI	>6.0, for PI<20% 4.0 – 5.0, for 35%<PI<65%	Stroud, 1974**
London Clay Formation (Thames Group)	$S_{u,UU} = f_1 \cdot N_{60}$ Where f_1 varies by PI	5.5 - 6.0 for 41%<PI<51%	White et al. 2019
Woolwich & Reading Formations (Lambeth Group),	$S_{u,UU} = f_1 \cdot N$ Where f_1 varies by PI	3.2 - 4.4, decreasing with PI	Stroud, 1974**
Gault Formation (Selborne Group)	$S_{u,UU} = f_1 \cdot N$	4.4	Nash et al. 1996**
Oxford Clay Formation (Ancholme Group)	$S_{u,UU} = f_1 \cdot N$ Where f_1 varies by PI	3.3 – 5.6, decreasing with PI	Stroud, 1974**
Whitby Mudstone Formation (Lias Group)	$S_{u,UU} = f_1 \cdot N$	4.0 (one result)	Stroud, 1974**
Mercia Mudstone Group*	$S_{u,UU} = f_1 \cdot N_{60}$ For insensitive weak rocks	5.0	Stroud, 1989**

*Note: Re-named from Keuper Marl according to the British Geological Survey Lexicon, (BGS,2020).
**Note: tests prior to BS EN ISO 22476-3:2005+A1:2011

Table 2: A summary of soil laboratory testing data and SPT data for samples from 96 boreholes in the Oxford Clay Formation (OXC_w), Whitby Mudstone Formation (WHM_w) and Charmouth Mudstone Formation ($CHAM_w$)

Formation (Group) [a]	Number of UU triaxial tests with SPT data [b,c]	Number of UU triaxial tests with soil classification and SPT data [b,c,d]
Oxford Clay (Ancholme Group)	70	21
Whitby Mudstone (Lias Group)	12	1
Charmouth Mudstone (Lias Group)	53	26
TOTAL	**135**	**48**

[a] British Geological Survey Lexicon, (BGS,2020). [b] Unconsolidated undrained triaxial tests on 100 mm diameter samples to BS1377-7:1990. [c] SPT to BS EN ISO 22476-3:2005+A1:2011 and assuming +/-1m offset distance. [d] Tested to BS1377-2:1990 and BS EN ISO 17892-1:2014

Table 3: Descriptive statistics for the UU triaxial test data and SPT data from the Oxford Clay Formation (OXC_w), Whitby Mudstone Formation (WHM_w) and Charmouth Mudstone Formation ($CHAM_w$).

Geological Formation	Number of pairs	Undrained shear strength (kPa)			SPT N_{60}-value		
		Mean	**Standard deviation**	**COV (%)**	**Mean**	**Standard deviation**	**COV (%)**
Oxford Clay	70	109	48	44	25	12	48
Whitby Mudstone	12	101	43	42	28	14	51
Charmouth Mudstone	53	111	47	42	29	11	39

Table 4: Fitting coefficients for the SPT N_{60} -value (explanatory variable) and undrained shear strength of the Oxford Clay Formation, Whitby Mudstone Formation and Charmouth Mudstone Formation samples using (i) linear regression through the origin and (iii) a Gaussian probability density function (PDF) fitted to the data.

Geological Formation	N	Mean coefficient (f_1 or $f_{p,\mu}$)	Standard deviation (σ)	$f_{p,5}$	$f_{p,95}$	COV (%)	MAPE (%)	Model range
Single coefficient								
Oxford Clay	70	3.58	N/A	N/A	N/A	55	55	$12 < N_{60} < 59$
Whitby Mudstone	12	2.98	N/A	N/A	N/A	55	51	$12 < N_{60} < 58$
Charmouth Mudstone	53	3.71	N/A	N/A	N/A	36	28	$12 < N_{60} < 54$
Gaussian PDF coefficient								
Oxford Clay	70	4.91	2.54	0.74	9.08	52	N/A	$0 < f_p < 12$
Whitby Mudstone	12	N/A	N/A	N/A	N/A	N/A	N/A	N/A
Charmouth Mudstone	53	4.09	1.33	1.90	6.28	32	N/A	$1 < f_p < 8$

Figures

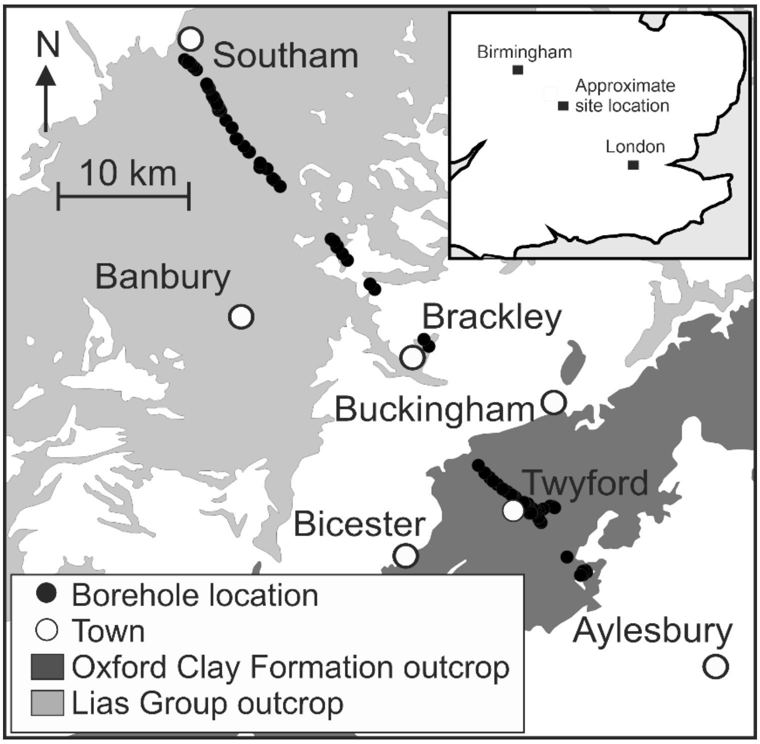

Figure 1: The borehole locations, nearby towns and cities in relation to outcrops of Oxford Clay (Ancholme Group), Charmouth Mudstone Formation and Whitby Mudstone Formation (Lias Group). Contains British Geological Survey materials © UKRI 2025.

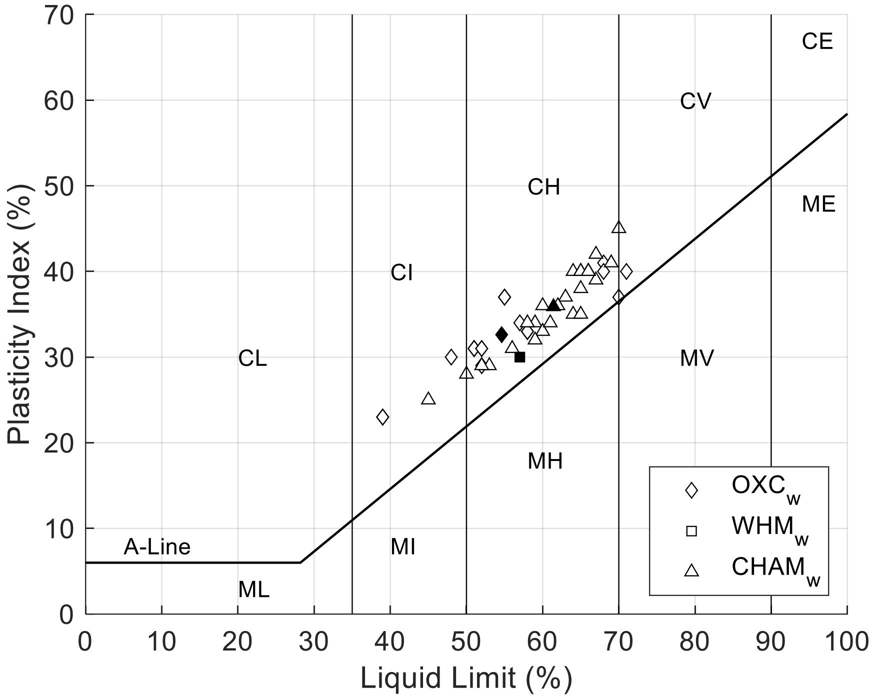

Figure 2: A Casagrande plot showing the plasticity results for triaxial samples with associated SPT and soil classification data, categorised by formation. Values for weathered clays from the Oxford Clay Formation (OXC_w), Whitby Mudstone Formation (WHM_w) and Charmouth Mudstone Formation ($CHAM_w$) are shown. Mean values are shown as black symbols. Samples with SPT N_{60} –values < 12 were omitted.

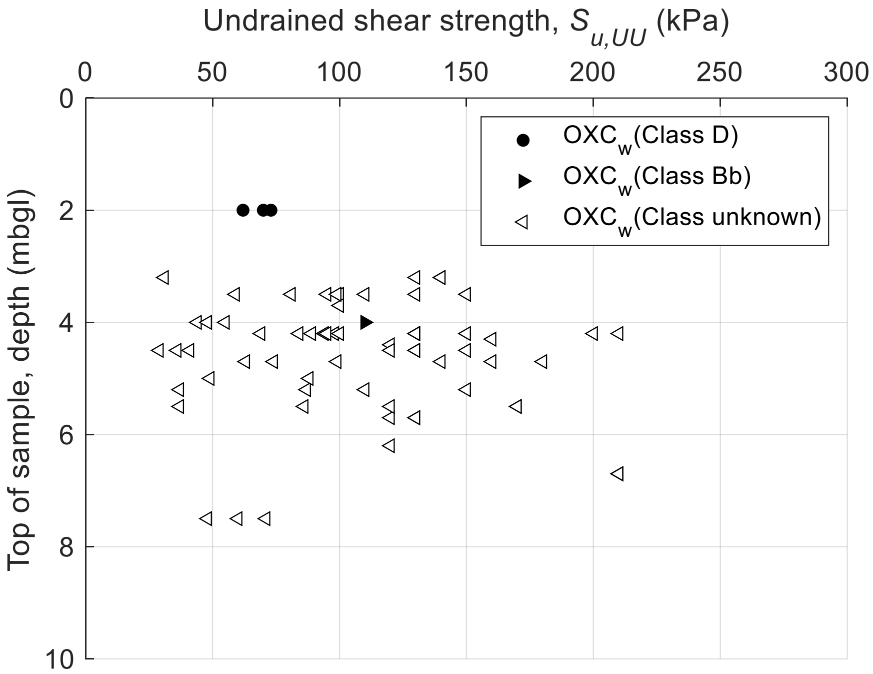

(a)

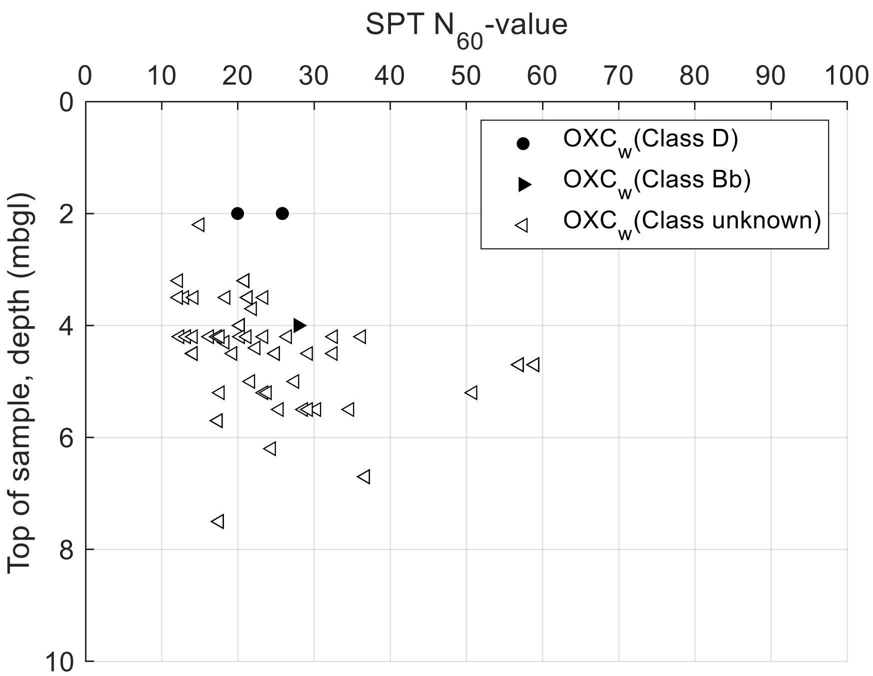

(b)

Figure 3: ***Profiles for the 70 weathered Oxford Clay Formation (OXCw) samples*** *showing (a) the undrained shear strength (kPa) of the triaxial samples and (b) the N_{60}-values of the associated SPT test. The weathering class is also shown.*

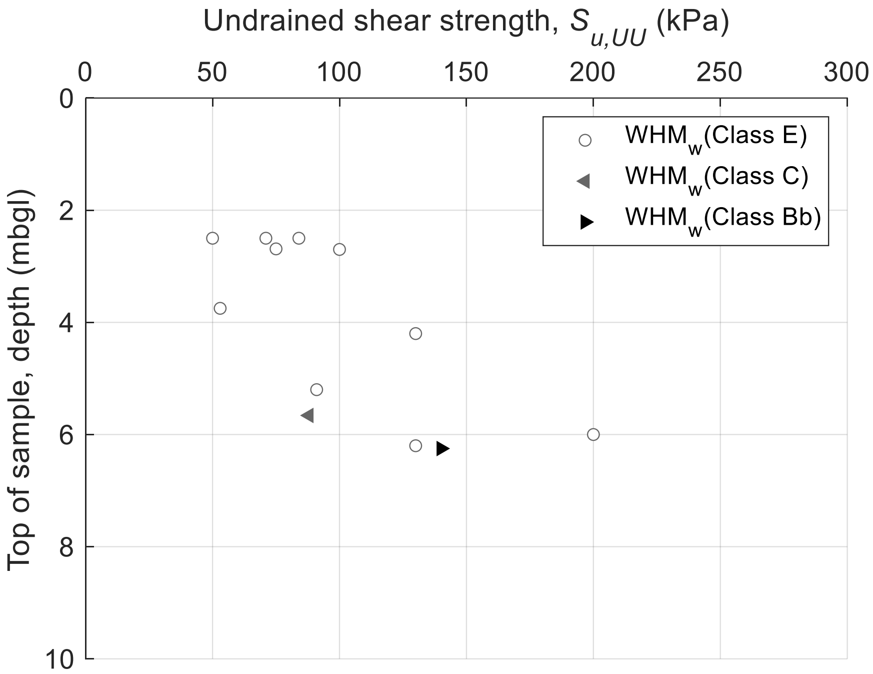

(a)

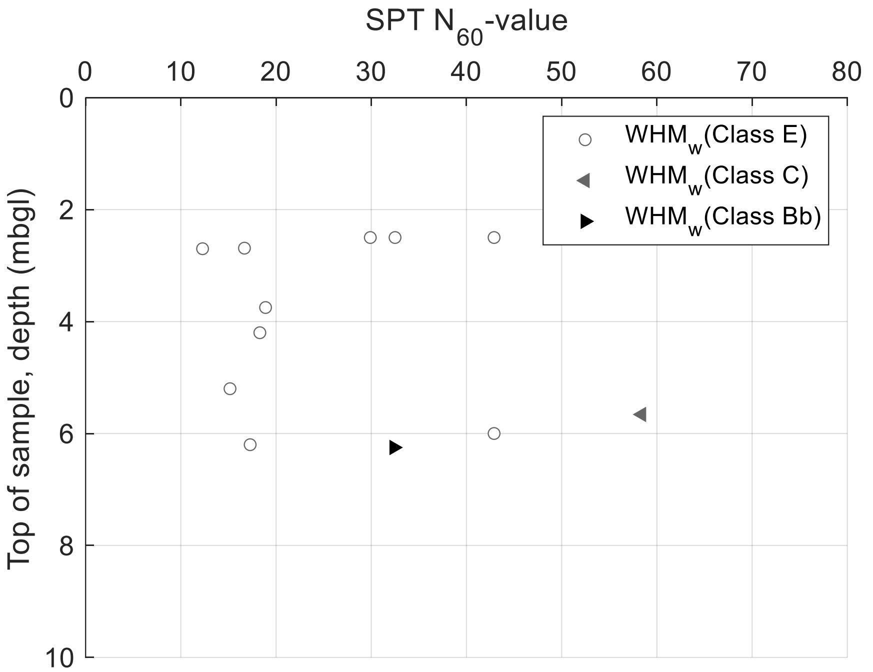

(b)

Figure 4: Profiles for the 12 weathered Whitby Mudstone Formation (WHM_w) samples showing (a) the undrained shear strength (kPa) of the triaxial samples and (b) the N_{60}-values of the associated SPT tests. The weathering class is also shown.

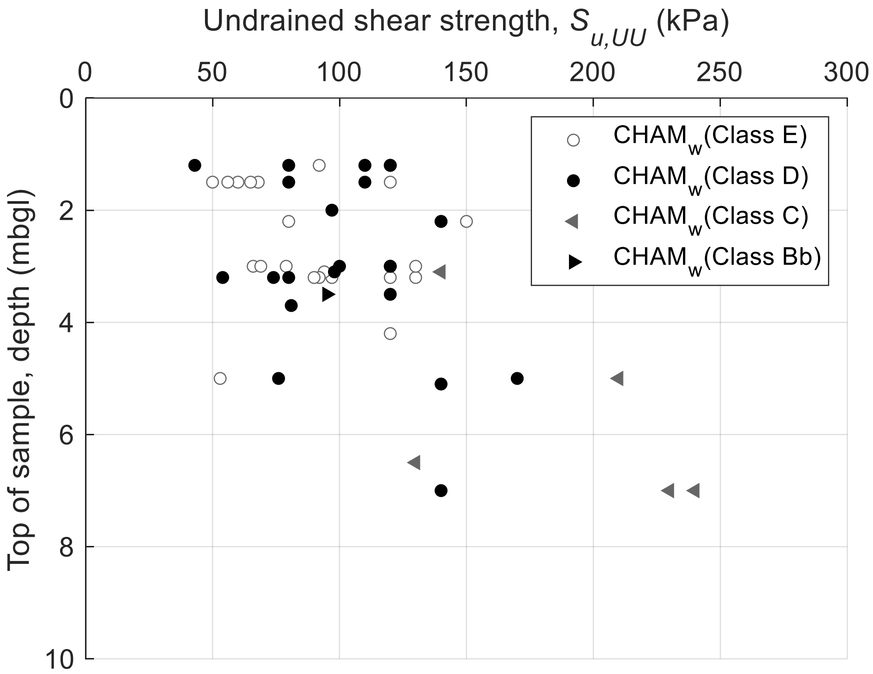

(a)

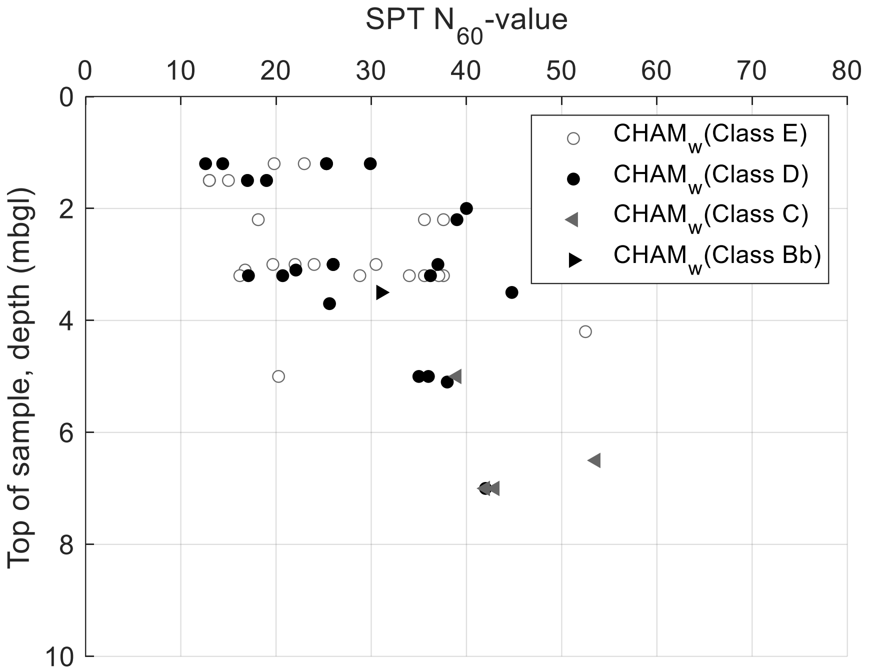

(b)

Figure 5: Profiles for the 53 weathered Charmouth Mudstone Formation (CHAM$_w$) samples showing (a) the undrained shear strength (kPa) of the triaxial samples and (b) the N_{60}-values of the associated SPT tests. The weathering class is also shown.

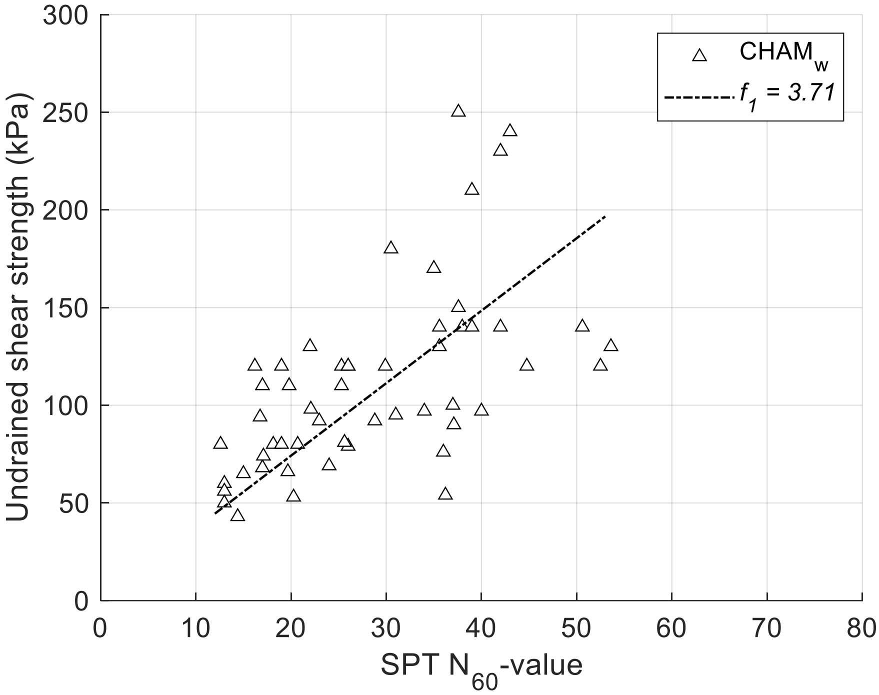

CHAMw
f1 = 3.71
Undrained shear strength (kPa)
SPT N60-value
0
50
100
150
200
250
300
0
10
20
30
40
50
60
70
80

(a)

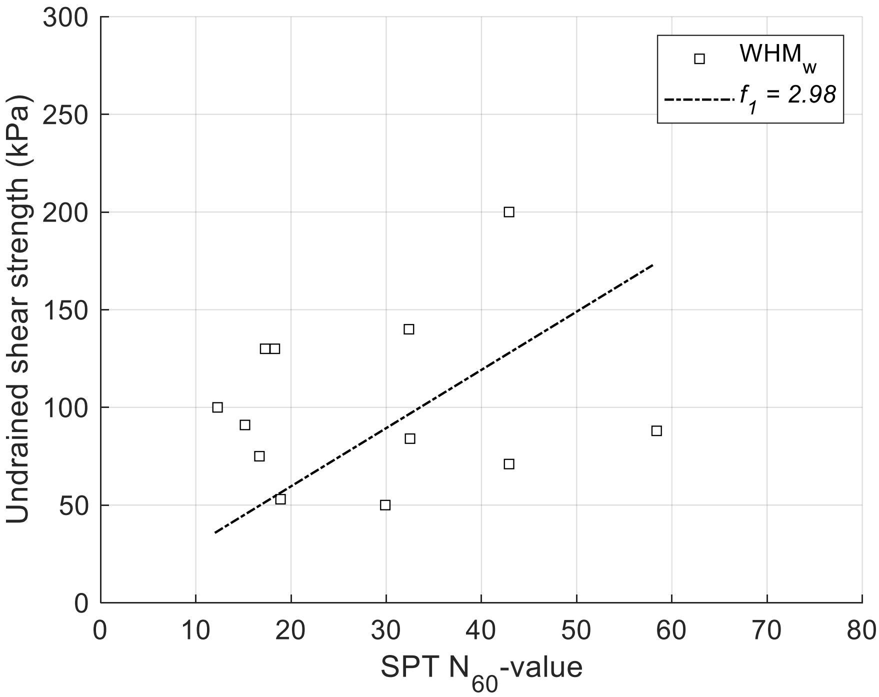

WHMw
f1 = 2.98
Undrained shear strength (kPa)
SPT N60-value
0
50
100
150
200
250
300
0
10
20
30
40
50
60
70
80

(b)

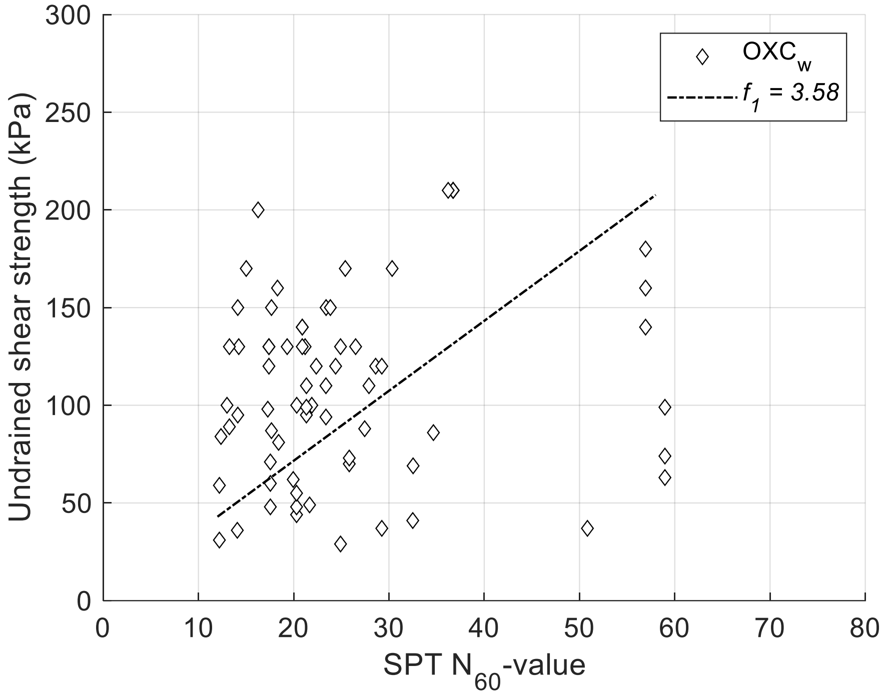

(c)

Figure 6: SPT N_{60}-values compared to the undrained shear strength (kPa) of associated, rotary cored samples. Results and regression trend lines through the origin are shown for the (a) Oxford Clay Formation (OXC_w)(n=70), (b) Whitby Mudstone Formation (WHM_w)(n=12) and (c) Charmouth Mudstone Formation ($CHAM_w$)(n=53). SPT N_{60} –values < 12 were omitted from the analyses. The regression coefficient (f_1) for each formation is shown.

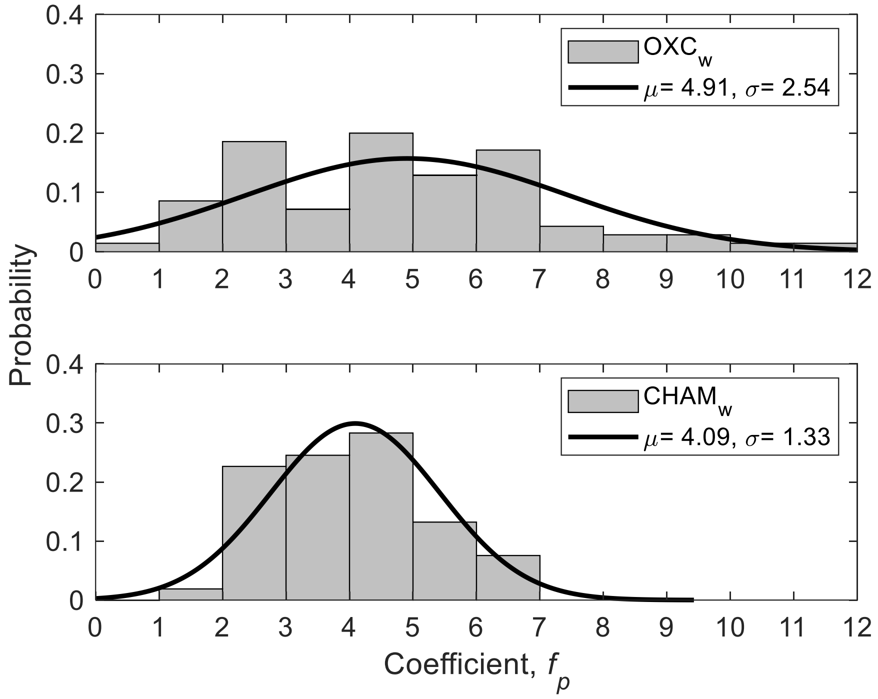

Figure 7: The probability density and Gaussian probability density functions for the coefficient (f_p) in weathered clays of the Oxford Clay Formation (OXC_w)(n=70) and Charmouth Mudstone Formation ($CHAM_w$)(n=53). The mean (μ) and standard deviation (σ) of the Gaussian probability density functions are shown. The COV values are shown in Table 4.

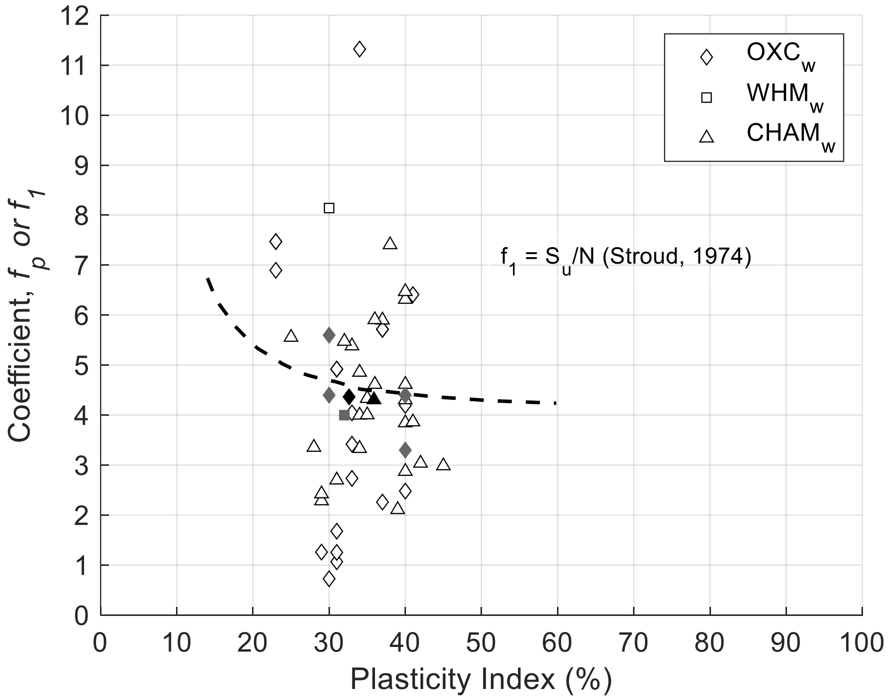

Figure 8: Coefficients for individual SPT and triaxial pairs (f_p) compared to plasticity index for weathered clays of the Oxford Clay Formation (OXC_w)(n=21), Whitby Mudstone Formation (WHM_w)(n=1) and Charmouth Mudstone Formation ($CHAM_w$)(n=26). Mean coefficients ($f_{p,\mu}$) for OXC_w and $CHAM_w$ are shown in black. Mean coefficients (f_1) measured by Stroud (1974) are shown in grey.

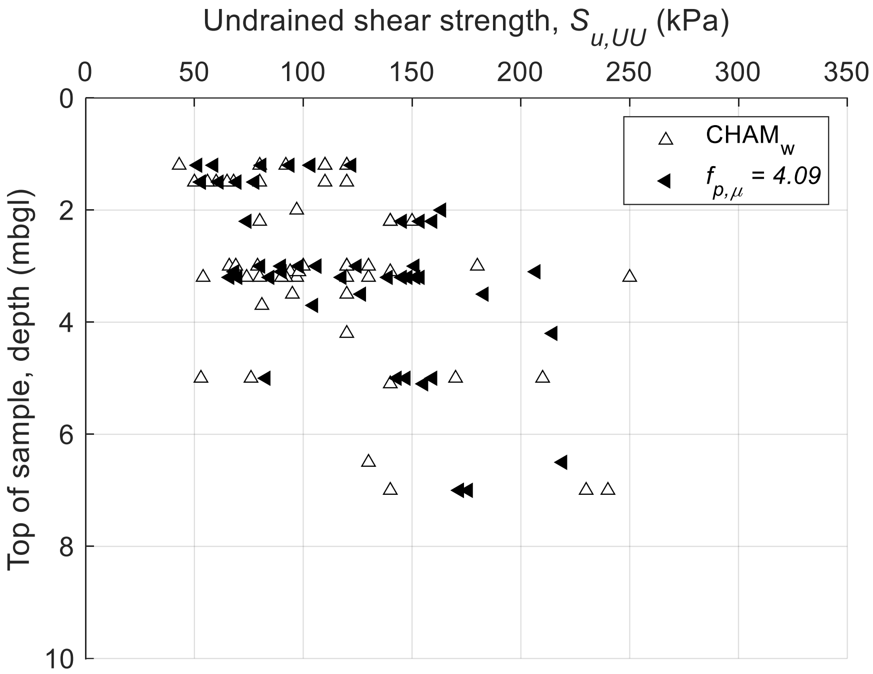

(a)

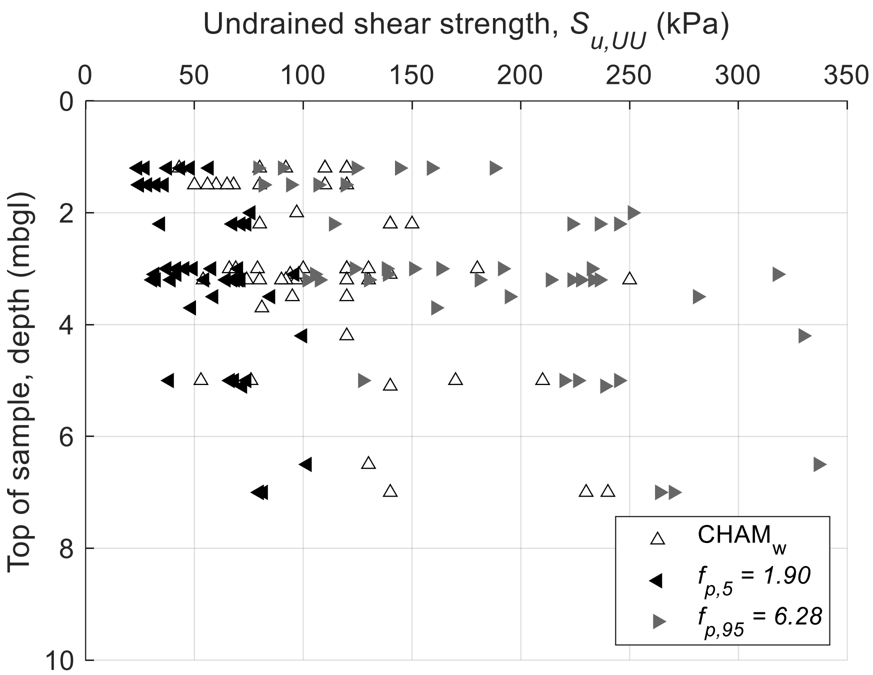

(b)

Figure 9: Undrained shear strength from the 53 weathered Charmouth Mudstone Formation ($CHAM_w$) triaxial samples, compared with undrained shear strength derived from 53 SPT N_{60}-values, using Equation 4 with (a) a mean average coefficient, ($f_{p,\mu}$) and (b) a 5th percentile ($f_{p,5}$) and 95th percentile ($f_{p,95}$) coefficient.